remote sensing

MDPI

Article

An Information Entropy-Based Sensitivity Analysis of Radar Sensing of Rough Surface

Yu Liu and Kun-Shan Chen *

The State Key Laboratory of Remote Sensing Science, Institute of Remote Sensing and Digital Earth, Chinese Academy of Sciences, Beijing 100101, China; liuyu@radi.ac.cn

* Correspondence: chenks@radi.ac.cn; Tel.: +86-010-64848730

Received: 31 December 2017; Accepted: 8 February 2018; Published: 12 February 2018

Abstract: We apply Shannon entropy, an information content measure, in sensitivity analysis (SA), stemming from the fact that the essence of SA is to preserve the maximum information content of the parameters of interest that are inverted from the radar response. Then, the sensitivity to the observation configuration and surface parameters is subsequently analyzed. Attempts are also made to explore advantages, by maximizing the information content, of dual-polarization and multi-angle in improving the parameter retrieval from radar sensing of rough surface. Simulation results show that the entropy is a good indicator of the sensitivity of the radar response to the surface parameter, as it contains information on not only the probability distribution of the scattering coefficient but also on its deviation. By information entropy, richer details, to large extent, on the scattering behavior are offered through quantitatively predicting the scattering signal saturation, evaluating the effect of using multi-polarization and multi-angle observation configuration, and identifying non-significant variables. It is found that Shannon entropy, compared to Renyi entropy, appears to better represent the sensitivity with respect to monotonic variation and narrower parameter ranges. The proposed entropy-based SA method helps to deepen our understanding of the microwave scattering behavior in response to surface parameters.

Keywords: radar sensing; sensitivity analysis; backscattering; information theoretic criterion

1. Introduction

Parameter sensitivity analysis (SA) of electromagnetic waves scattering from a randomly rough surface is pivotal in the field of remote sensing of surface geometrical and dielectric parameters [1–3]. For example, it is common to retrieve the geophysical parameters of interest, such as soil moisture and roughness, from the scattering measurements [4–7], based on analyzing the sensitivity of the scattering behavior and mechanisms. Additionally, by knowing the scattering patterns, one could effectively avoid undesired parameters, while accordingly devising a means to retrieve the parameters of interest.

One of the critical issues in the estimation of surface parameters from radar responses is that the surface parameters, including surface roughness (*rms* height and correlation length) and dielectric constant, are strongly coupled under a certain set of radar parameters (wavelength, incident angle and polarization) [4–8]. Therefore, it has been both theoretically and practically motivated to conduct a parameter SA to determine an optimal observation configuration and to determine an appropriate approach for sensing and decoupling, to an optimal level, the surface roughness and dielectric constant.

There have been numerous studies concerning SA for scattering behavior from rough surfaces. Most of them employ partial derivative-based approaches, e.g., the studies by Chen et al. [9], Mao et al. [10], and Brogioni et al. [11]. These studies generally focus on the average impact of the input factors on the model outputs, and show difficulty, to certain extent, in accurately coming up with the sensitivity when the model input is uncertain or when the model is nonlinear [12,13].

For a random rough surface, it becomes a firm and indisputable fact that the scattering response varies nonlinearly with the surface conditions. Furthermore, there is a well-known problem of uniqueness in the radar response measurement, partly due to the complex wave–target interactions, and partly because of uncertainty sources, such as the random characteristics of rough surface and noise-corrupted radar echoes [9]. Thus, their uncertainties must be resolved, or at least quantified, before parameter retrieval algorithms can be applied with known and acceptable accuracy in surface observations.

Recently, global-based SA methods, such as extended Fourier amplitude sensitivity test (EFAST) [14–21] and Sobol's method [22–24], have begun to consider the probability distribution functions of parameters as prior knowledge in examining changes in the model response. However, these methods often suffer difficulty in illustrating SA variations for specific surface conditions or observational configurations, which is essential in establishing surface sensing algorithms. Moreover, they are always based on a uniformly distributed sampling of input parameters, which results in questionable validity in practical predictions of the random processes involved in rough surface scattering [25] as well as the radar returns that are embedded in a noisy background, which are probabilistic in nature. In addition, it is found that the parameter ranges affect both the sensitivity indexes and their relative importance, and the different parameter intervals exhibit different sensitivities [15], which can produce uncertainty in the interpretation of the importance of the parameters and may be misleading in the parameter selection. Thus, a more essential approach that considers both the derivatives as well as the scattering response distributions is expected to improve the SA that is required to meet a given surface condition's retrieval accuracy specification.

The goal of SA is to preserve the maximum information content of the parameters of interest, which are transferred from inputs to outputs of the radar response. Therefore, we attempt to adopt information theory, originally developed by Shannon [26], to characterize the information content in terms of communications theory, to quantitatively and objectively evaluate the information of the sensor configurations and to evaluate observational uncertainty that is associated with parameter sampling.

To the best of our knowledge, SA on microwave scattering from rough surface using information theoretic criteria is not yet available in the literature. Apparently, quantitative and systematic insights from information theory into rough surface scattering properties should be attempted to explore the potential sensing capabilities.

The objective of this paper can be summarized as follows: (1) introduce information theory in the SA of scattering from rough surfaces; (2) provide a comprehensive SA of the surface parameters and observation geometries; and (3) conduct an intensive investigation exploring the potential advantage of using dual-polarization and multi-angle in improving rough surface sensing.

Section 2 firstly briefly outlines the rough surface scattering simulation and the data model of radar measurements, and then introduces the method of applying information theoretic criteria in SA of scattering from rough surfaces. Section 3, the main body of this paper, analyzes the parameter sensitivity dependence of rough surface and radar configurations from extensive scattering simulations. Section 4 discusses the proposed information-based SA approach. Potential applications of dual-polarization and multi-angle are also given. Finally, in Section 5, conclusions are drawn to close the paper.

2. Materials and Methods

2.1. Surface Scattering Model

(1) Radar Scattering Coefficients

Referring to the geometry of scattering in Figure 1, supposed a plane wave impinges onto a dielectric rough surface which scatters waves up into the incident plane and down into the lower medium, with the electric and magnetic fields been written as

$$\vec{E}^i = \hat{p}E_0 \exp\left[-j\left(\vec{k}_i \cdot \vec{r}\right)\right] \tag{1}$$

$$\vec{H}^i = \frac{1}{\eta}\hat{k}_i \times \vec{E}^i \tag{2}$$

where $j = \sqrt{-1}$; $\hat{p}$ is the unit polarization vector; E_0 is the amplitude of the incident electric field; and η the intrinsic impedance of the upper medium. The wavenumber plane in incident and scattering directions are defined as follows, respectively [1].

$$\begin{aligned} &\vec{k}_i = k\hat{k}_i = \hat{x}k_{ix} + \hat{y}k_{iy} + \hat{z}k_{iz}; \\ &k_{ix} = k\sin\theta_i\cos\phi_i, k_{iy} = k\sin\theta_i\sin\phi_i, k_{iz} = k\cos\theta_i \end{aligned} \tag{3}$$

$$\begin{aligned} &\vec{k}_s = k\hat{k}_s = \hat{x}k_{sx} + \hat{y}k_{sy} + \hat{z}k_{sz}; \\ &k_{sx} = k\sin\theta_s\cos\phi_s, k_{sy} = k\sin\theta_s\sin\phi_s, k_{sz} = k\cos\theta_s \end{aligned} \tag{4}$$

For linearly horizontal-polarized and vertical-polarized waves, the polarization vector $\hat{p}$, for incident and scattering waves, is defined as

$$\begin{aligned} &\hat{h}_i = -\hat{x}\sin\phi_i + \hat{y}\cos\phi_i \\ &\hat{v}_i = \hat{h}_i \times \hat{k}_i = -(\hat{x}\cos\theta_i\cos\phi_i + \hat{y}\cos\theta_i\sin\phi_i + \hat{z}\sin\theta_i) \\ &\hat{h}_s = \hat{\phi} = -\hat{x}\sin\phi_s + \hat{y}\cos\phi_s \\ &\hat{v}_s = \hat{\theta} = \hat{h}_s \times \hat{k}_s = \hat{x}\cos\theta_s\cos\phi_s + \hat{y}\cos\theta_s\sin\phi_s - \hat{z}\sin\theta_s \end{aligned} \tag{5}$$

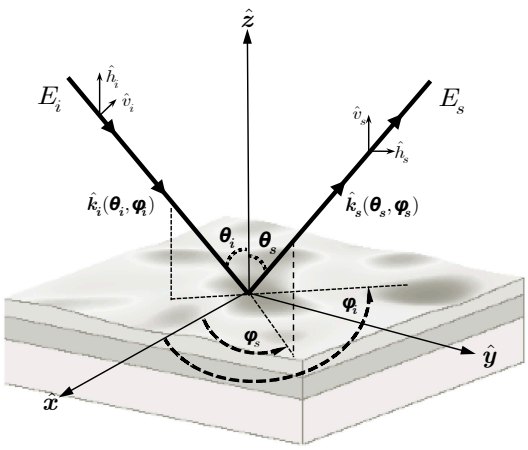

Figure 1. A geometry of rough surface scattering.

For backscattering, which is the focus of this study, the incident azimuth angle ϕ_i is set to zero, and scattering angle is $\left(\theta_s = \theta_i, \phi_i = 180^\circ\right)$.

In this paper, an Advanced Integral Equation Model (AIEM) is adopted as a working model for numerical simulations of backscattering coefficient from rough surface. The detail description concerning the model can be seen in papers by Chen et al. [27], Wu et al. [28] and Chen et al. [29].

(2) Surface Parameters

The range of parameters we used in this study is listed in Table 1. The dielectric coefficient relating to the moisture content is obtained using Dobson model [30,31] which is a mixed dielectric constant model. Moreover, we focused on the L-band (i.e., 1.26 GHz) as it shows good sensitivity to moisture content found in numerous studies.

Table 1. Simulation surface and radar parameters.

Parameters			Range
Surface Parameter	ks	Normalized root mean surfaces height	0.01~2
	kl	Normalized correlation length	0.01~10
	m_v	Moisture content (m^3m^{-3})	0.01~0.45
Radar Parameter	θ_i	Incident angle	10°~70°
	θ_s	Scattering angle	$=\theta_i$
	φ_s	Scattering azimuthal angle	180°

Note: Exponential correlation function was used in all cases.

(3) Data Model of Radar Measurements

A proper data model is to enable a mapping of measurement space to parameter space in which we are of interest. Here, we detail the procedures. The radar backscattering from a rough surface can be mathematically modeled as Chen et al. [32].

$$\mathbf{y} = \mathbf{A}\mathbf{x} + \mathbf{u} \tag{6}$$

where $\mathbf{x}$ is the surface parameters vector; matrix $\mathbf{A}$ relates the surface parameters vector $\mathbf{x}$ to radar scattering coefficients $\mathbf{y}$; and $\mathbf{u}$ represents the measurement error vector induced by system and calibration errors, and speckle noise. Note that the radar response is formed by, in general, the scattering matrix. For the purpose of this paper, and without loss of generality, we assume it is formed by multi-polarized scattering coefficients:

$$\mathbf{y} = [\sigma^o_{hh}, \sigma^o_{hv}, \sigma^o_{vv}]^{\mathrm{t}} \tag{7}$$

The surface parameters of interest are the normalized *rms* height ks, correlation length kl, and moisture content m_v that is related to dielectric constant [30,31], where k is wavenumber:

$$\mathbf{x} = [ks, kl, m_v]^{\mathrm{t}} \tag{8}$$

When it comes to estimation and perhaps to filtering as well, the measurement Equation (1) takes the form for one-step time or sample n in framework of adaptive filtering such as Kalman filter:

$$\mathbf{y}_n = \mathbf{A}\mathbf{x}_n + \mathbf{u}_n, \tag{9}$$

where the subscript n denotes the measurement at a discrete nth time or sample step. The process equation relates the transition states of the surface parameters vector x:

$$\mathbf{x}_{n+1} = \Phi_n \mathbf{x}_n + \mathbf{B}_n \mathbf{v}_n, \tag{10}$$

where Φ_n is a transition matrix, $\mathbf{v}_n$ is the process error vector, and $\mathbf{B}_n$ is the error matrix.

2.2. Information Theoretic Criteria

In this section, we first briefly introduced information theoretic criteria. Then, its relationship with data distributions parameters is analyzed with a purpose of application in SA of microwave scattering from rough surface.

(1) Information Theoretical Analysis

Shannon entropy, a measure of information content, can be used to characterize the amount of information that we obtain when we observe the result of an experiment. Moreover, the entropy can also be interpreted as a measure of uncertainty because it is numerically equal to the amount of uncertainty contained in the outcome of an experiment before it is conducted [26,33]. It has been

widely used in various models and applications, such as engineering design [34], network anomaly detection [35] and species distribution modeling [36].

Considering that the goal of SA is to preserve the maximum information content of the parameters, and that there exists uncertainty in the scattering process of a random surface, we attempt to introduce the concept of entropy into our SA of microwave scattering. It is natural to measure the information as a first step, using entropy, which is a measure of unpredictability of information content [26]. We aim to observe the entropy and mutual coherence among the parameters. This scheme enables us to quantify and objectively evaluate how sensitive the output is to the input variable (surface roughness and dielectric constant).

Considering that there are many entropy criteria, we shall start with two widely used criteria, Shannon entropy (SE) [26] and Renyi entropy (RE) [33], which are defined as

$$\mathrm{SE} = \mathcal{E}[\mathrm{I}(\mathbf{y})] = \mathcal{E}[-\ln(P(\mathbf{y}))] \tag{11}$$

$$\mathrm{RE} = \frac{1}{1-\alpha}\log[\mathcal{E}(P^{\alpha-1}(\mathbf{y}))] \tag{12}$$

where $\mathcal{E}$ is an expected value operator; I is Hartley's information content of observation vector $\mathbf{y}$; and P is the probability density function (pdf). Note that SE is a special case of RE, i.e., it is the limit of RE as $\alpha = 1$. In this study, we adopt the quadratic entropy, which is the RE when $\alpha = 2$.

In practice, we use the Parzen method [37] with a Gaussian kernel G to estimate the pdf in Equation (12), arriving at

$$H_r(\mathbf{b}) = -\log[\frac{1}{N^2}\sum_{i=1}^{N}\sum_{j=1}^{N} G(y_i - y_j, \sigma^2)] \tag{13}$$

where y_i are components of $\mathbf{y}$. The base of the log function can be 2, e, or 10. In this study, the natural (e-based) log is used.

(2) Relationship between Information Entropy and Data Parameters

To explore the performance of the entropy in SA, we begin by looking into its relationship to the distribution of parameters, including the probabilistic distribution and the standard deviation σ. For probability distributions, the skewness, γ, and excess kurtosis, κ, are used to indicate asymmetry and normality, respectively. These parameters are given as

$$\sigma = \sqrt{\left(\sum_{i=1}^{n}(x_i - \overline{x})^2\right)/n} \tag{14}$$

$$\gamma = \mathrm{E}(x-\mu)^3/\sigma^3 \tag{15}$$

$$\kappa = \mathrm{E}(x-\mu)^4/\sigma^4 - 3 \tag{16}$$

where μ is the mean of random variable x, σ measures statistical dispersion, γ measures the asymmetry of the data around the sample mean and κ indicates how outlier-prone a distribution is. Thus, γ and κ for a normal distribution are zero. If γ is negative, the data are spread out more to the left of the mean than to the right. Distributions that are more outlier-prone than the normal distribution have positive κ, with negative values of κ indicating distributions that are less outlier-prone than the normal distribution.

In this study, seven typical probability distributions, namely, uniform, exponential, normal, beta, Weibull, Lognormal, and Gamma distribution, were generated. Their distribution parameters and corresponding entropies are given Table 2, and their probability distributions are presented in Figure 2. It was observed that the entropy, both SE and RE, has a close relationship with the distribution parameters. Overall, high entropy always corresponds to a normal-like distribution whose γ and κ are

close to 0.0. It decreases for a greater deviation from the normal distribution, which is characterized by asymptotic and normality. Moreover, for most distributions, a greater standard deviation σ always corresponds to greater entropy. Thus, it can be inferred that the output parameter is expected to be non-sensitive if the input parameter is disturbed normally, and the output parameter deviates greatly from the normal distribution and has a small σ. It is not difficult to understand this phenomenon, because, if the input is decentralized, a sensitive system is expected to have a decentralized output, while an insensitive system tends to be centralized, which can be reflected by a large amount of asymmetry and a normal probabilistic distribution, with small dispersion. Therefore, the entropy can be used as an indicator of the SA because it reflects not only the data deviation but also the probability distribution, which is also given by its definition in Equations (11) and (12).

Table 2. The distribution parameters of seven typical distributions and their entropy.

Distribution	Equation [1]	Number	Parameters	γ	κ	σ	SE (nat)	RE (nat)
Uniform		Case 1	$a = 0.0, b = 0.1$	0.01	−1.18	0.57	3.75	3.76
Exponential	$y = f(x\|\mu) = e^{x/\mu}/\mu$	Case 2	$\mu = 2.0$	1.90	5.59	1.99	3.42	3.28
Normal	$y = f(x\|\mu,\sigma) = \frac{1}{\sigma\sqrt{2\pi}} e^{\frac{-(x-\mu)^2}{2\sigma^2}}$	Case 3	$\mu = 2.0, \sigma = 0.125$	−0.01	0	0.13	3.88	3.78
		Case 4	$\mu = 2.0, \sigma = 0.25$	−0.02	0.17	0.25	3.90	3.76
		Case 5	$\mu = 2.0, \sigma = 1.25$	0.00	−0.03	1.25	3.88	3.77
Beta	$y = f(x\|a,b) = \frac{1}{B(a,b)} x^{a-1}(1-x)^{b-1} I_{(0,1)}(x)$ [2]	Case 6	$a = 2.0, b = 0.125$	−3.30	11.86	0.14	1.47	−0.23
		Case 7	$a = 2.0, b = 0.25$	−2.03	3.8	0.18	2.66	1.77
		Case 8	$a = 2.0, b = 1.0$	−0.59	−0.55	0.23	3.77	3.67
Weibull	$y = f(x\|a,b) = ba^{-b}x^{b-1}e^{-\left(\frac{x}{a}\right)^b} I_{(0,\infty)}(x)$	Case 9	$a = 2.0, b = 0.25$	0.61	0.21	0.33	3.90	3.74
		Case 10	$a = 2.0, b = 1.25$	−0.61	0.45	0.11	3.90	3.72
		Case 11	$a = 2.0, b = 2.5$	−0.84	1.14	0.06	3.84	3.73
Lognormal	$y = f(x\|\mu,\sigma) = \frac{1}{x\sigma\sqrt{2\pi}} e^{\frac{-(\ln x-\mu)^2}{2\sigma^2}}$	Case 12	$\mu = 2.0, \sigma = 0.06$	0.18	0.08	0.47	3.88	3.78
		Case 13	$\mu = 2.0, \sigma = 0.25$	0.86	1.33	1.96	3.86	3.72
		Case 14	$\mu = 2.0, \sigma = 0.50$	1.56	3.45	4.38	3.63	3.56
Gamma	$y = f(x\|a,b) = x^{a-1}e^{\frac{x}{b}}/(b^a\Gamma(a))$	Case 15	$a = 2.0, b = 0.25$	1.33	2.47	0.35	3.69	3.58
		Case 16	$a = 2.0, b = 1.0$	1.36	2.7	1.76	3.64	3.61

[1] μ is the mean; γ, κ, and σ are skewness, kurtosis and standard deviation, respectively; [2] $B(.)$: Beta function. $I_{(0,1)}$ ensures that only the values in the range (0–1) have nonzero probability.

To further explore the entropy performance and determine suitable criteria, we compared the two entropy parameters, SE and RE, as a function of the data distribution parameters, for both the beta and normal distribution, with denser generated samples, as shown in Figure 3. The reason that we chose those two distributions lies in that field-measured rough surface parameters are always random normal distributed. In addition, the scattering response distributions are more likely to be those distributions when the inputs are normally distributed, which would be discussed in Section 3.1. In the figure, it can be seen that, for the beta distribution, SE increases with increasing σ while the absolute value of the γ and κ decreases, as expected. Similar results can be found for the normal distribution, except for the γ and κ, which are approximately 0, due to the function for generating simulation data.

Moreover, it is interesting to find that, of the two entropy parameters, the SE can provide a better representation of the sensitivity with respect to a monotone variation and sometimes a linear relationship with the distribution parameters, in addition to having the narrow range of 0.0–4.0. The RE fluctuates, and could have some extremely anomalous high value, as shown in Figure 3a,c,e. In Figure 3b,d we also see very weak dependences of entropy on γ and κ for Normal distribution, compared to Beta distribution. Therefore, in the following section, we choose SE as the indicator of SA.

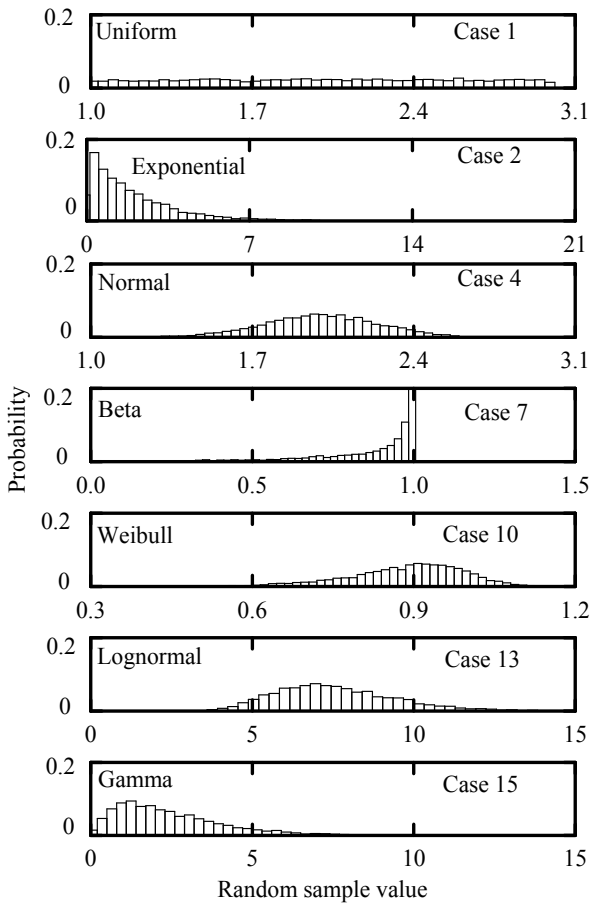

Figure 2. Seven typical probability distributions. Case *n* (*n* = 1, 2, 4, 7, 13, and 15) corresponds to the case in Table 1.

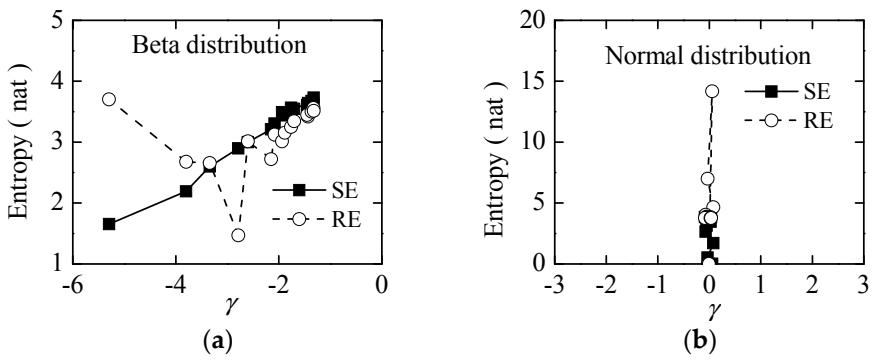

Figure 3. *Cont.*

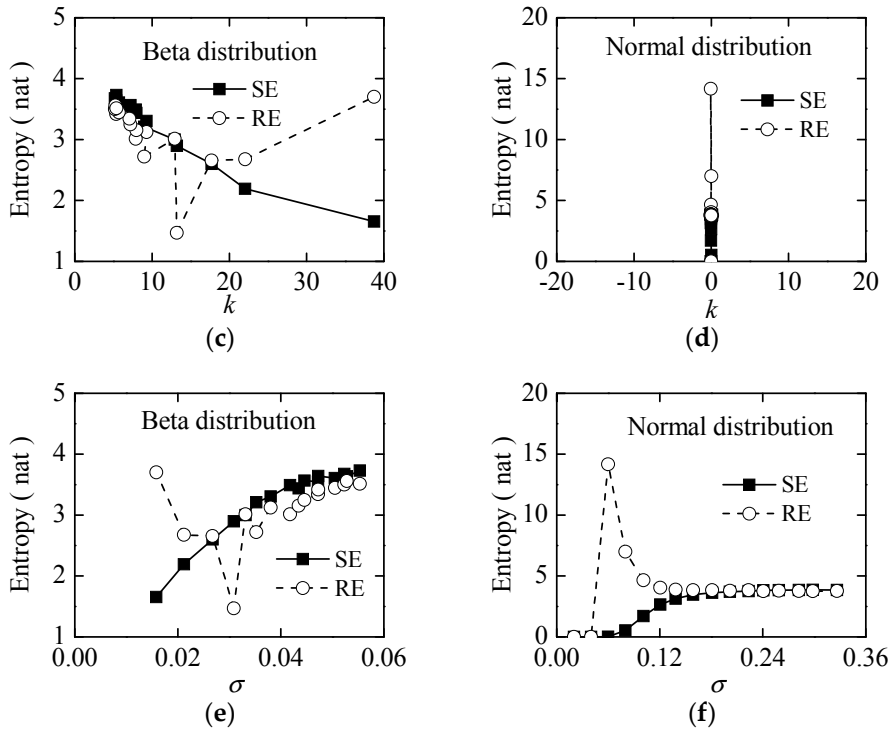

Figure 3. Renyi entropy (RE) and Shannon entropy (SE) as a function of the distribution parameters of: (**a**,**b**) γ; (**c**,**d**) κ; and (**e**,**f**) σ, for: (**a**,**c**,**e**) Beta distribution, $a = 20$; $b = 0.1, 0.1, \cdots, 1.6$; and (**b**,**d**,**f**) Normal distribution, $\mu = 30; \sigma = 0.02, 0.04, \cdots, 0.32$.

(3) Application of Information Entropy in SA of Scattering from Rough Surface

For the experiment, the procedure was divided into three parts: input data sampling, SE calculation, and sensitivity analysis. In the input data sampling part, we generate normal distributed random samples that involve surface parameters and incident angles. In this paper, 1000 samples were generated. The standard deviation, σ, was estimated to assess the uncertainty caused by system noise and the scattering properties of the random rough surfaces. Next, the parameters associated with each sample are fed into the AIEM model to obtain the backscattering coefficients and the corresponding entropy. Finally, the sensitivity to the surface condition and the observation configuration are analyzed comprehensively. Notice that, in this paper, we consider linear scale for radar signals.

3. Results

3.1. SA of Surface Condition

(1) Distribution Response of the Backscattering Coefficient

Figure 4 is scattering coefficient distribution with the normal disturbed rough surface parameter as inputs. The exponential correlation function is used at an incident angle of 45°. In the figure, we can see that, for dry and smooth surface, the scattering coefficient remains normal distributed. With increasing surface roughness and moisture content, the behavior of the rough surface scattering is not normally distributed, as is frequently assumed. It is more likely to be Beta distribution, as shown in Figure 5, and referring to Figure 2. This disagreement can be described by the departures of the γ and κ of returns from normal distribution counterparts. Moreover, we can see that, compared to surface with varying kl and m_v, the scattering response deviation is more obvious when varying ks. Finally, it can be observed that the HH-polarized distribution response is generally similar, but not exactly the same, as the VV-polarized ones.

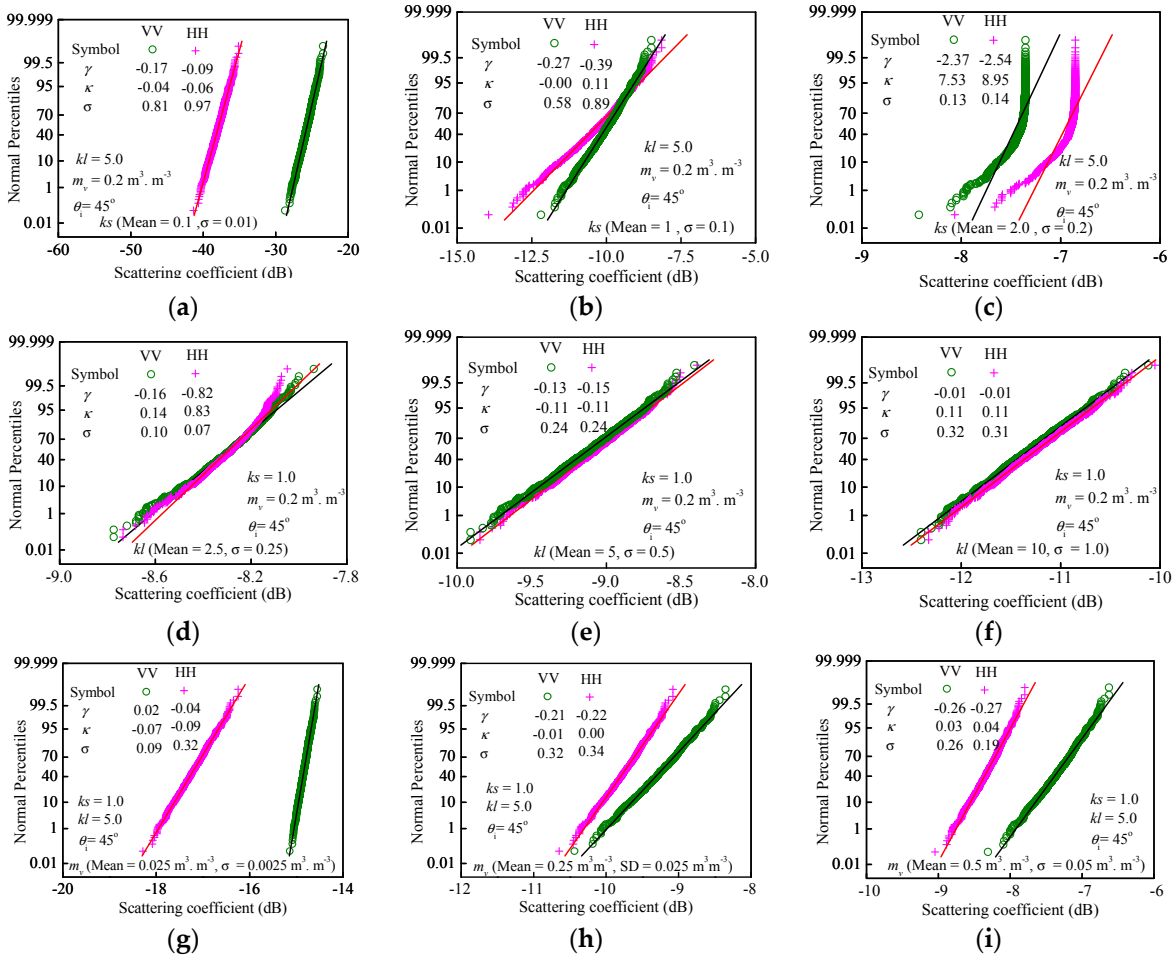

Figure 4. Probability of the scattering coefficient with normal distributed input surface parameters of: (**a**–**c**) ks; (**d**–**f**) kl; and (**g**–**i**) m_v, at the incident angle of 45°. The solid line is the reference line for a normal distribution fit. (**a**,**d**,**g**) Small ks, kl, and m_v; (**b**,**e**,**h**) medium ks, kl, and m_v; and (**c**,**f**,**i**) large ks, kl, and m_v. The parameters on upper left of the figures show the distribution of the scattering coefficients, while on the bottom are the input parameters.

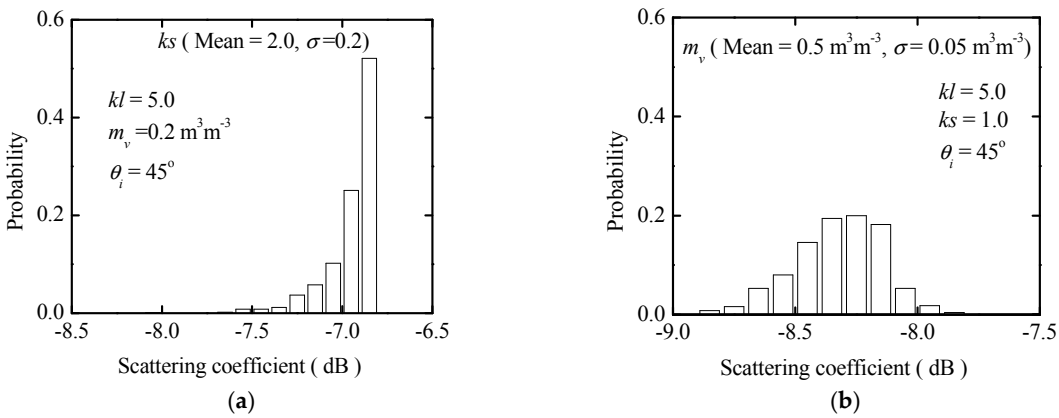

Figure 5. Probability distribution response of backscattering for rough surface with: (**a**) great roughness; and (**b**) high water content.

(2) SA by Information Entropy

Figure 6 is a volumetric slice of SE with three key surface parameters, namely, ks, kl, and m_v in the x, y, z directions, respectively. In the figure, we observe that the entropy related to the HH polarization is generally similar to that of VV polarization. Moreover, the backscattering signals were found to be more sensitive to ks than to m_v and kl. Those results are highly consistent with those by other methods, such as EFAST methods [15,16]. The consistency between the different models indicates again the feasibility of the proposed entropy-based method in SA.

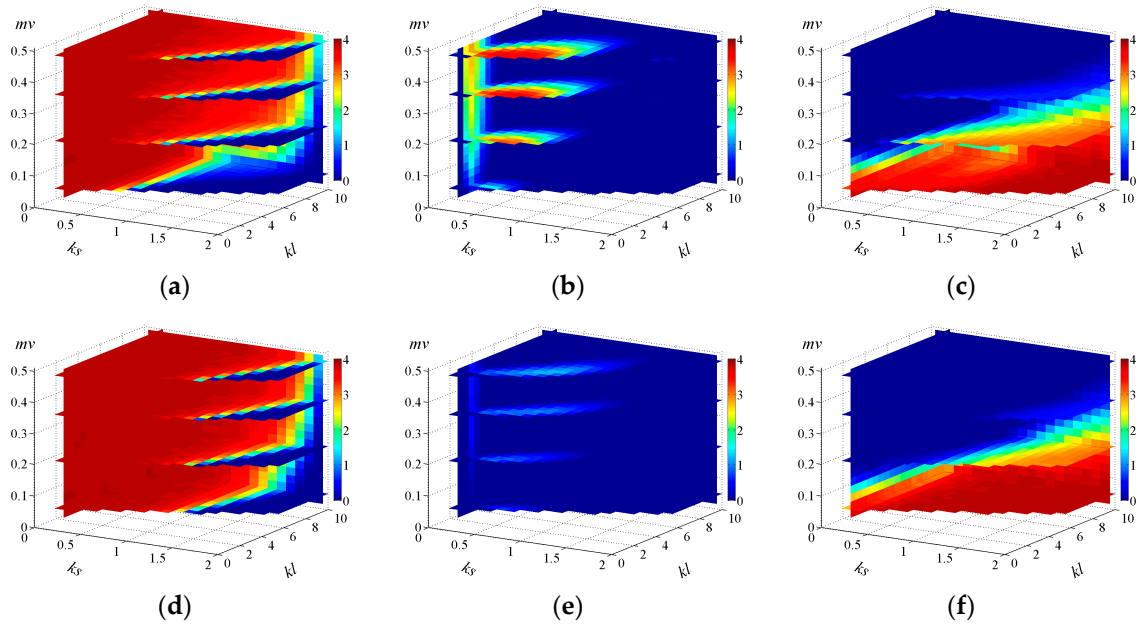

Figure 6. SE response to rough surface when varying: (**a**,**d**) ks; (**b**,**e**) ; and (**c**,**f**) m_v at a polarization of: (**a**–**c**) VV; and (**d**–**f**) HH. The incident angle is 45° and the frequency is 1.26 GHz. Normal distribution disturbances were added to the input parameters, with σ equal to 1% of the maximum of the corresponding surface parameters. As an example, σ is set to 0.02, 0.1, and 0.005 $m^3 m^{-3}$ when varying: (**a**,**d**) ks; (**b**,**e**) kl; and (**c**,**f**) m_v, respectively.

Note that, compared to other SA methods, the proposed entropy-based method can provide specific and detailed parameter sensitivity under various rough surface conditions, while there is always only single SA data for global-based methods or limited data for local-based method. Therefore, the proposed method can give us more insight into the scattering behaviors of rough surface and, thus, ensure better use of microwave scattering data in surface monitoring.

Another interesting finding is that it is easy to determine the saturation point of backscattering signals in the form of rapidly decreasing entropy. For example, it can be seen that backscattering signals tend to saturate for a rougher surface, and wet soil prompts the saturation.

3.2. Sensitivity of Observation Configuration

Figure 7 shows the distribution parameters and entropy as a function of the incident angles. The figure shows that, when the incident angle increases, for surfaces with different values of ks, the γ and σ decrease first and then increase, while the κ increases first and then increases. The turning points of those parameters are almost at the same incident angle. Correspondingly, the SE decreases first and then increases, and the smallest entropy is always found around the small incident angles for a smooth surface, and it shifts toward a greater incident angle for rougher cases. This finding indicates that, for roughness sensing, the backscattering observation at greater incident angles is preferable

for a smooth surface, while smaller incident angles for rough surfaces, with the aim of retaining the maximum information.

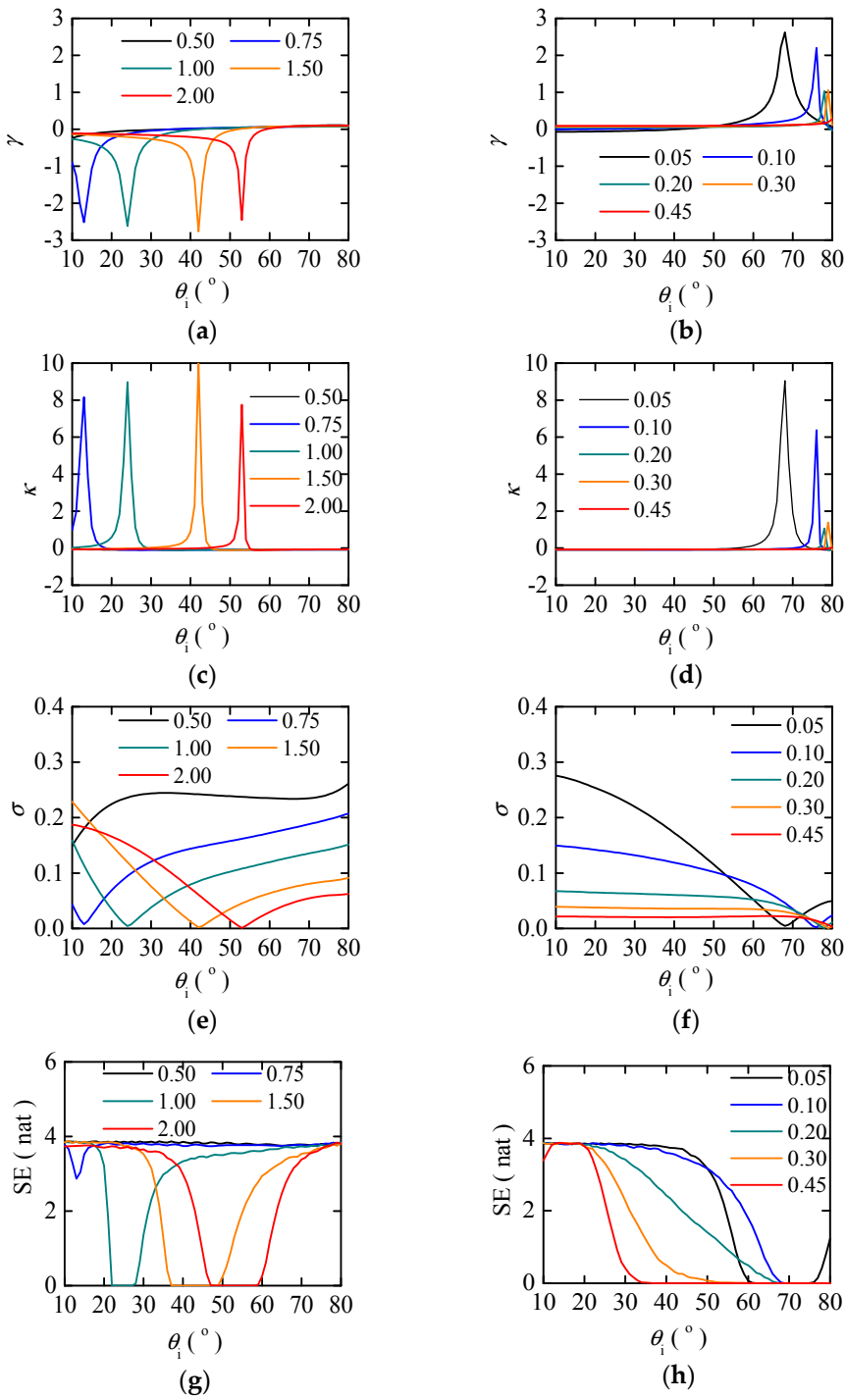

Figure 7. Distribution response and corresponding SE as a function of incident angles for varying: (**a**,**c**,**d**,**g**) ks. $kl = 5.0$, $m_v = 0.2$ m$^3m^{-3}$; and (**b**,**d**,**f**,**h**) m_v. $ks = 1.0$, $kl = 5.0$; and (**a**,**b**) γ; (**c**,**d**) κ; (**e**,**f**) σ; and (**g**,**H**) SE. Normally distributed inputs are the same as those in Figure 5.

For the moisture content, it is interesting to note that the distribution of m_v is notably different from that of ks. For example, a surface with a varying m_v has a negative γ, while it is positive when varying ks. The distribution response for a smooth surface with a small ks does not vary with incident angle, while a similar phenomenon can be found for a wet surface with high m_v. The turning point of

the distribution parameters always appears at larger incident angles ($> 60^{\circ}$) for various values of m_v, while it is at smaller incident angles for rough surfaces ($< 60^{\circ}$) for various ks. In addition, the SE curve with varying ks shows monotone, and the scattering signal saturation appears earlier for a wet surface, while it is funnel-shaped, and the scattering signal saturation dip shift is greater at incident angles with roughness.

The above results are based on VV polarization. Similar analyses with HH polarization indicate almost identical behavior.

3.3. SA of Dual-Polarization and Multi-Angle

Motivated by the different responses of the scattering signals from different polarizations, as shown in Figure 5, two sets of simulation data with dual-polarization are combined (i.e., the polarization ratio and the polarization difference), as given in Figure 8. The figure shows that dual-polarization is expected to provide some improvements in estimating the moisture content compared to single-polarized measurements by reducing the scattering coefficient saturation for rough and wet surfaces, which is a problematic issue in surface parameter retrieving.

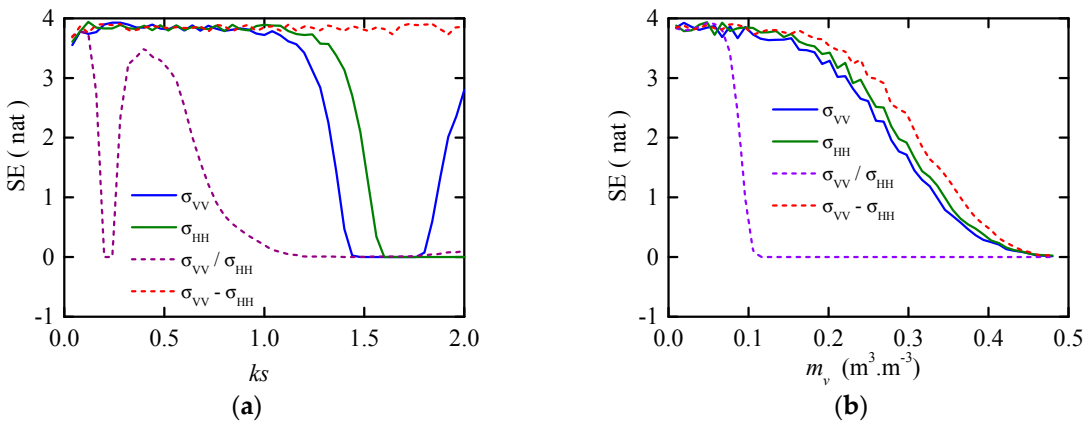

Figure 8. SE of single- and dual-polarization for varying: (**a**) ks. $kl = 5.0, m_v = 0.2$ m$^3 m^{-3}$; and (**b**) m_v. $ks = 1.0,\ kl = 5.0$ at $\theta_i = 45^{\circ}$.

For multi-angle observations, we investigate the SE response of two angles ($\theta_i = 30^{\circ}, 45^{\circ}$), and three angles ($\theta_i = 30^{\circ}, 45^{\circ}, 50^{\circ}$) in simulations, as shown in Figure 9. Note that only varying the roughness ks and moisture content m_v were considered because the scattering response to kl is comparatively less sensitive, as stated in Section 3.1. The figure shows that a multi-angle observation can help to address the issue of the scattering signal saturation for wet and rough surfaces, which is similar to the using dual-polarization. Moreover, it is interesting to note that for multi-angle, which is the combination of backscattering coefficients at two incident angles ($\sigma_{VV(30^{\circ})}/\sigma_{VV(45^{\circ})}$), the SE is sensitive to ks but not to m_v, while the combination of three angles ($\left(\sigma_{VV(30^{\circ})}\right)^2 / \left(\sigma_{VV(45^{\circ})}\sigma_{VV(50^{\circ})}\right)$) shows sensitivity to both ks and m_v. This finding implies that one can use the ratio between the values of the backscatter data at two angles to estimate the roughness while assigning the soil moisture a constant value. The soil moisture can then be estimated based on the ratio of the three backscatter values using the estimated roughness. Note that there is an obvious SE dip for a multi-angle observation due to the almost equal scattering coefficients of those angles.

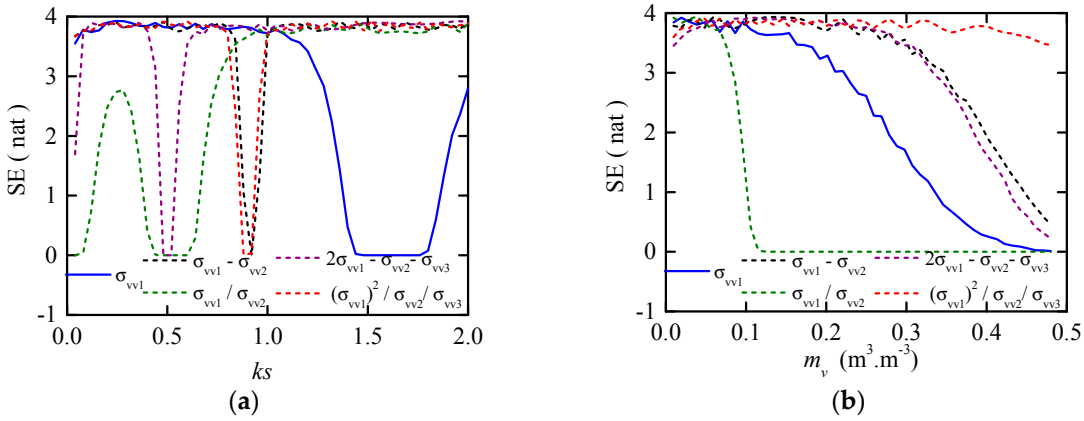

Figure 9. SE of the single and multi-angle when varying: (**a**) ks. $kl = 5.0, m_v = 0.2\,\mathrm{m^3m^{-3}}$; and (**b**) m_v. $ks = 1.0$, $kl = 5.0$. σ_{VVi} is the VV-polarized scattering coefficient with the incident angle $\theta_i = 30^\circ, 45^\circ, 50^\circ$.

4. Discussion

In Figures 4 and 5, we start with exploring the distribution response of the backscattering coefficient under different bare surface conditions with the normal disturbed rough surface parameter. We can see that, for rough and wet surface, scattering returns does not agree with the frequently assumed normal distribution, and is more likely to be Beta distribution. Therefore, scattering distribution response should be considered carefully to reduce the uncertainty in rough surface sensing.

To further indicate the sensitivity of radar response to surface parameters, we use information entropy because it not only reflects probabilistic distribution, but also the deviation. In Figure 6, we find that the entropy-based SA results are highly consistent with those by other methods, such as EFAST methods [15,16]. The consistency between the different models indicates again the feasibility of the proposed entropy-based method in SA. Moreover, compared to other SA methods, the entropy-based method can provide specific and detailed parameter sensitivity under various rough surface conditions, while there is always only single SA data for global-based methods or limited data for local-based method. Another interesting finding is that it is easy to determine the saturation point of backscattering signals in the form of rapidly decreasing entropy. Therefore, the proposed method can give us more insight into the scattering behaviors of rough surface and, thus, ensure better use of microwave scattering data in surface monitoring.

Considering that the scattering's response to the incident angles and polarization are of great interest in optimizing the radar system designs, we analyze the scattering sensitivity as a function of incident angles in Figure 7. The different distributions and entropy responses to the roughness and moisture content in terms of the incident angles and polarization imply a different degree of sensitivity, and thus, multiple incident angles and polarizations can help improve accuracy of the retrieval of parameters.

We then combine simulation data with dual-polarization and multi-angle, as shown in Figures 8 and 9. The results indicate that the entropy-based SA can estimate visually the advantage of multi-polarization and multi-angle, and combining multi-polarization and multi-angle could help to decouple the effect of the moisture content and roughness on the scattering observations.

5. Conclusions

In this paper, we applied SE in SA of scattering from rough surface, and comprehensively analyzed the sensitivity to observation configuration and surface parameters including surface roughness (*rms* height, correlation length) and moisture content. Attempts were also made to explore, by maximizing the information content, the potential advantages of duel-polarization and multi-angle

in improving retrieval of surface parameters from radar sensing. The results show that information entropy is a good indicator of sensitivity of radar response to surface parameters because it not only reflects probabilistic distribution, but also the deviation. By information entropy, richer details on scattering behavior is offered through evaluating in detail the parameter sensitivities, predicting quantitatively the scattering signal saturation, estimating visually the advantage of multi-polarization and multi-angle, and identifying non-significant variables, similar to normal SA attempts. Moreover, compared to Renyi entropy, Shannon entropy seems to better represent the sensitivity with respect to monotone variation and narrower data range. From the sensitivity analysis, it is therefore confirmed, on a more theoretically solid ground, that measurement from multi-polarization and multi-angle greatly helps alleviate the saturation of scattering coefficient at rougher and wetter surface, and even has the potential to decouple the effect of moisture content and roughness on surface observation. Thus, the entropy-based SA offers to deepen our understanding of the microwave scattering behavior, and, as such, to devise an effective retrieval of moisture content from radar measurements.

Acknowledgments: This work was supported in part by the National Natural Science Foundation of China under grants 41531175, and in part the Director General's Innovative Funding-2015, and Youth Funding-2016 of the Institute of Remote Sensing and Digital Earth, Chinese Academy of Sciences.

Author Contributions: Kun-Shan Chen and Yu Liu conceived and designed the experiments; Yu Liu performed the experiments; Yu Liu analyzed the data; Kun-Shan Chen and Yu Liu contributed analysis tools; and Yu Liu wrote the paper.

Conflicts of Interest: The authors declare no conflict of interest.

References

1. Ulaby, F.T.; Long, D.G. *Microwave Radar and Radiometric Remote Sensing*; University of Michigan Press: Ann Arbor, MI, USA, 2014.
2. Crosson, W.L.; Limaye, A.S.; Laymon, C.A. Parameter sensitivity of soil moisture retrievals from airborne L-band radiometer measurements in SMEX02. *IEEE Trans. Geosci. Remote Sens.* **2005**, *43*, 1517–1528. [CrossRef]
3. Du, Y.; Ulaby, F.T.; Dobson, M.C. Sensitivity to soil moisture by active and passive microwave sensors. *IEEE Trans. Geosci. Remote Sens.* **2000**, *38*, 105–114. [CrossRef]
4. Zribi, M.; Dechambre, M. A new empirical model to retrieve soil moisture and roughness from C-band radar data. *Remote Sens. Environ.* **2003**, *84*, 42–52. [CrossRef]
5. Verhoest, N.E.; Lievens, H.; Wagner, W.; Álvarez-Mozos, J.; Moran, M.S.; Mattia, F. On the soil roughness parameterization problem in soil moisture retrieval of bare surfaces from synthetic aperture radar. *Sensors* **2008**, *8*, 4213–4248. [CrossRef] [PubMed]
6. Lievens, H.; Verhoest, N.E.; De Keyser, E.; Vernieuwe, H.; Matgen, P.; Álvarez-Mozos, J.; De Baets, B. Effective roughness modeling as a tool for soil moisture retrieval from C-and L-band SAR. *Hydrol. Earth Syst. Sci.* **2011**, *15*, 151–162. [CrossRef]
7. Zribi, M.; Gorrab, A.; Baghdadi, N. A new soil roughness parameter for the modelling of radar backscattering over bare soil. *Remote Sens. Environ.* **2014**, *152*, 62–73. [CrossRef]
8. Bindlish, R.; Jackson, T.J.; Wood, E.; Gao, H.; Starks, P.; Bosch, D.; Lakshmi, V. Soil moisture estimates from TRMM Microwave Imager observations over the Southern United States. *Remote Sens. Environ.* **2003**, *85*, 507–515. [CrossRef]
9. Chen, K.S.; Yen, S.K.; Huang, W.P. A simple-model for retrieving bare soil-moisture from radar-scattering coefficients. *Remote Sens. Environ.* **1995**, *54*, 121–126. [CrossRef]
10. Mao, K.B.; Tang, H.J.; Zhang, L.X.; Li, M.C.; Guo, Y.; Zhao, D.Z. A method for retrieving soil moisture in Tibet region by utilizing microwave index from TRMM/TMI data. *Int. J. Remote Sens.* **2008**, *29*, 2903–2923. [CrossRef]
11. Brogioni, M.; Pettinato, S.; Macelloni, G.; Paloscia, S.; Pampaloni, P.; Pierdicca, N.; Ticconi, F. Sensitivity of bistatic scattering to soil moisture and surface roughness of bare soils. *Int. J. Remote Sens.* **2010**, *31*, 4227–4255. [CrossRef]

12. Saltelli, A.; Ratto, M.; Andres, T.; Campolongo, F.; Cariboni, J.; Gatelli, D.; Saisana, M.; Tarantola, S. *Global Sensitivity Analysis: The Primer*; John Wiley & Sons: West Sussex, UK, 2008.
13. Wagner, S. Global sensitivity analysis of predictor models in soft- ware engineering. In Proceedings of the International Workshop on Predictor Models in Software Engineering, Minneapolis, MN, USA, 20–26 May 2007; p. 3.
14. Petropoulos, G.; Srivastava, P.K. (Eds.) *Sensitivity Analysis in Earth Observation Modelling*; Elsevier: Oxford, UK, 2016.
15. Ma, C.F.; Li, X.; Wang, S.G. A global sensitivity analysis of soil parameters associated with backscattering using the advanced integral equation model. *IEEE Trans. Geosci. Remote Sens.* **2015**, *53*, 5613–5623.
16. McNairn, H.; Jackson, T.J.; Wiseman, G.; Belair, S.; Berg, A.; Bullock, P.; Colliander, A.; Cosh, M.H.; Kim, S.B.; Magagi, R.; et al. The soil moisture active passive validation experiment 2012 (SMAPVEX12): Prelaunch calibration and validation of the SMAP soil moisture algorithms. *IEEE Trans. Geosci. Remote Sens.* **2015**, *53*, 2784–2801. [CrossRef]
17. Wang, J.; Li, X.; Lu, L.; Fang, F. Parameter sensitivity analysis of crop growth models based on the extended Fourier amplitude sensitivity test method. *Environ. Model. Softw.* **2013**, *48*, 171–182. [CrossRef]
18. Estrada, V.; Diaz, M.S. Global sensitivity analysis in the development of first principle-based eutrophication models. *Environ. Model. Softw.* **2010**, *25*, 1539–1551. [CrossRef]
19. Li, D.; Jin, R.; Zhou, J.; Kang, J. Analysis and reduction of the uncertainties in soil moisture estimation with the L-MEB model using EFAST and ensemble retrieval. *IEEE Geosci. Remote Sens. Lett.* **2015**, *12*, 1337–1341.
20. Lentini, N.E.; Hackett, E.E. Global sensitivity of parabolic equation radar wave propagation simulation to sea state and atmospheric refractivity structure. *Radio Sci.* **2015**, *50*, 1027–1049. [CrossRef]
21. Neelam, M.; Mohanty, B.P. Global sensitivity analysis of the radiative transfer model. *Water Resour. Res.* **2015**, *51*, 2428–2443. [CrossRef]
22. Sobol, I.M. Sensitivity estimates for nonlinear mathematical models. *Math. Model. Comput. Exp.* **1993**, *1*, 407–414.
23. Sudret, B. Global sensitivity analysis using polynomial chaos expansions. *Reliab. Eng. Syst. Saf.* **2008**, *93*, 964–979. [CrossRef]
24. Saltelli, A.; Sobol, I.M. About the use of rank transformation in sensitivity of model output. *Reliab. Eng. Syst. Saf.* **1995**, *50*, 225–239.
25. Saltelli, A.; Annoni, P. How to avoid a perfunctory sensitivity analysis. *Environ. Model. Softw.* **2010**, *25*, 1508–1517. [CrossRef]
26. Shannon, C.E. A mathematical theory of communication. In *ACM SIGMOBILE Mobile Computing and Communications Review*; ACM: New York, NY, USA, 2001; Volume 5, pp. 3–55.
27. Chen, K.S.; Wu, T.D.; Tsang, L.; Li, Q.; Shi, J.C.; Fung, A.K. Emission of rough surfaces calculated by the integral equation method with comparison to three-dimensional moment method simulations. *IEEE Trans. Geosci. Remote Sens.* **2003**, *41*, 90–101. [CrossRef]
28. Wu, T.D.; Chen, K.S.; Shi, J.C.; Lee, H.W.; Fung, A.K. A study of AIEM Model for Bistatic Scattering from Randomly Surfaces. *IEEE Trans. Geosci. Remote Sens.* **2008**, *46*, 2584–2598.
29. Chen, K.L.; Chen, K.S.; Li, Z.L.; Liu, Y. Extension and validation of an advanced integral equation model for bistatic scattering from rough surfaces. *Prog. Electromagn. Res.* **2015**, *152*, 59–76. [CrossRef]
30. Dobson, M.C.; Ulaby, F.T.; Hallikainen, M.T.; El-Rayes, M.A. Microwave dielectric behavior of wet soil—Part II. Dielectric mixing models. *IEEE Trans. Geosci. Remote Sens.* **1985**, *1*, 35–46. [CrossRef]
31. Peplinski, N.R.; Ulaby, F.T.; Dobson, M.C. Dielectric-properties of soils in the 0.3–1.3-GHz range. *IEEE Trans. Geosci. Remote Sens.* **1995**, *33*, 803–807. [CrossRef]
32. Chen, K.S.; Wu, T.D.; Shi, J.C. A model- based inversion of rough surface parameters from radar measurements. *J. Electromagn. Waves Appl.* **2001**, *15*, 173–200. [CrossRef]
33. Rényi, A. On measures of entropy and information. In Proceedings of the Fourth Berkeley Symposium on Mathematical Statistics and Probability, Berkeley, CA, USA, 20 June–30 July 1960; Volume 1, pp. 547–561.
34. Liu, H.; Chen, W.; Sudjianto, A. Relative entropy based method for probabilistic sensitivity analysis in engineering design. *J. Mech. Des.* **2006**, *128*, 326–336. [CrossRef]
35. Ziviani, A.; Gomes, A.T.A.; Monsores, M.L.; Rodrigues, P.S. Network anomaly detection using nonextensive entropy. *IEEE Commun. Lett.* **2007**, *11*, 1034–1036. [CrossRef]

36. Phillips, S.J.; Dudík, M.; Schapire, R.E. A maximum entropy approach to species distribution modeling. In Proceedings of the Twenty-First International Conference on Machine Learning, Banff, AB, Canada, 4–8 July 2004; ACM: New York, NY, USA, 2004; p. 83.
37. Parzen, E. On the estimation of a probability density function and the mode. *Ann. Math. Stat.* **1962**, *33*, 1065–1076. [CrossRef]